

1           Supplementary Information for: Impact of nonionic  
2           surfactants on the water activity of binary and ternary  
3                                   aqueous solutions

4                                   February 3, 2026

5   Emily K. Werner,<sup>1</sup> Owen Wasserlein,<sup>1</sup> Cassidy Mahan,<sup>1</sup> Andreas Zuend,<sup>2</sup> and  
6                                   Alison Bain<sup>1,\*</sup>

7                   1. Department of Chemistry, Oregon State University, Corvallis, Oregon, USA

8                   2. Department of Atmospheric and Oceanic Sciences, McGill University, Montreal, Quebec, Canada

9   \* Alison Bain

10 e-mail: [alison.bain@oregonstate.edu](mailto:alison.bain@oregonstate.edu)

## 11 Bulk-to-surface partitioning

12 Surfactants partition to interfaces, and in high surface-area-to-volume ratio systems, this  
13 can lead to a depleted surfactant concentration in the system bulk as the surface concentration  
14 becomes non-negligible. 8 mL samples for water activity measurements are placed in a cylindri-  
15 cal dish with a 1.5-inch (3.81 cm) diameter. If we assume the surfactant partitions only to the  
16 air-water interface, the surface-area-to-volume ratio of the sample is  $1.425 \text{ cm}^{-1}$ , and if we as-  
17 sume the surfactant can partition to the container interface as well, the surface-area-to-volume  
18 ratio of the sample is  $3.9 \text{ cm}^{-1}$ . These surface-area-to-volume ratios correspond to spherical  
19 droplets of radii 2.1 and 0.77 cm, respectively.

20 We use a simple kinetic partitioning scheme<sup>1,2</sup> to predict the depletion ratio in the sample  
21 bulk as a function of total surfactant concentration ( $c_{tot}$ ).

$$\frac{c_{bulk}}{c_{tot}} = \frac{1}{2} \left( 1 - \zeta - \frac{\zeta}{f} \right) + \frac{1}{2} \sqrt{\left( 1 - \zeta - \frac{\zeta}{f} \right)^2 + 4 \frac{\zeta}{f}} \quad (\text{S1})$$

$$f = \frac{\Gamma_{max} A K_{eq}}{V} \quad (\text{S2})$$

$$\zeta = \frac{\Gamma_{max} A}{c_{tot} V} \quad (\text{S3})$$

22 Here,  $c_{bulk}$  is the depleted bulk concentration,  $\Gamma_{max}$  and  $K_{eq}$  are the surfactant-dependent  
23 maximum surface excess and equilibrium partitioning constant determined from the Langmuir  
24 isotherm (taken from refs<sup>2,3</sup>),  $A$  is the surface area, and  $V$  is the volume.

25 Fig. S5 shows the predicted depletion ratio for Tween20, Triton X-100, and OTG in a 1 cm  
26 radius droplet. Changing the droplet size to 0.77 or 2.1 cm slightly changes the shape of the

27 curves in the low surfactant concentration region, but does not impact the total concentration  
28 where the depletion ratio reaches unity.

29 For Tween20 and Triton X-100, the stronger two surfactants, bulk-to-surface partitioning  
30 is expected to reduce the surfactant dissolved in the solution bulk by up to 4% at the lowest  
31 surfactant concentrations. When the surfactant critical micelle concentration (CMC) is reached,  
32 the loss of surfactant to the interface is expected to reduce the bulk concentration by less  
33 than 1%. For OTG, the weakest surfactant, bulk-to-surface partitioning is expected to reduce  
34 the bulk concentration by less than 0.5% over the full surfactant concentration range. At  
35 surfactant concentrations of 3 mM (corresponding to water mass fractions of 0.996, 0.998, and  
36 0.999 for Tween20, Triton X-100, and OTG, respectively), the depletion ratio is approximately  
37 unity for every surfactant. Therefore, at water mass fractions lower than 0.996, bulk-to-surface  
38 partitioning is not expected to significantly impact the total surfactant concentration in the  
39 sample bulk during water activity measurements, for any surfactant system investigated here.

## 40 **Surfactant hygroscopicity**

41 The hygroscopicity of each surfactant was determined by calculating the radial hygroscopic  
42 growth factor. Dry particles with a 50 nm radius were used in all calculations. The dry  
43 surfactant mass was then determined using the pure surfactant density (1100, 1070, and 999.8  
44 kg/m<sup>3</sup> for Tween20, Triton X-100, and OTG, respectively).<sup>4</sup> We assume that the change in  
45 droplet volume can be used to determine the volume, and thus mass of water added to the  
46 droplet, allowing the calculation of the surfactant mass fraction at each step. The radial growth  
47 factor is then calculated as the ratio of the wet particle diameter and the dry diameter. The  
48 equilibrium water activity predicted by AIOMFAC for each surfactant mass fraction was then

49 calculated. For Tween20 and Triton X-100, the oxyethylene subgroup description was used as  
50 it more closely agrees with the experimentally determined water activities.

51 The hygroscopicity  $\kappa$  was then determined at 95% RH for each surfactant.<sup>5</sup>  $V_{dry}$  is the dry  
52 particle volume and  $V_{water}$  is the volume of water added to the particle.

$$\frac{1}{a_w} = 1 + \kappa \frac{V_{dry}}{V_{water}} \quad (\text{S4})$$

Table S1: Organic subgroups from Fig. S2 used to define surfactant molecules for AIOMFAC calculations. Tween20 and Triton X-100 (1) use ether and alkyl groups to describe the hydrophilic tail, while Tween20 and Triton X-100 (2) use oxyethylene groups.

Subgroup	Tween20 (1)	Tween20 (2)	Triton X-100 (1)	Triton X-100 (2)	OTG
CH <sub>3</sub>	1	1	5	5	1
CH <sub>2</sub>	28	11	9	1	6
CH	4	4	–	–	1
C	–	–	2	2	–
ACH	–	–	4	4	–
AC	–	–	2	2	–
OH	3	3	1	1	4
CH <sub>2</sub> [OH]	3	3	1	1	1
CH[OH]	–	–	–	–	3
CH <sub>2</sub> O	21	5	9	1	1
CHO[ether]	–	–	–	–	1
CH <sub>2</sub> COO	1	1	–	–	–
CH <sub>2</sub> OCH <sub>2</sub> [oxyethylene]	–	16	–	8	–

Table S2:  $\kappa$  values for strong nonionic surfactants at 85, 90 and 95% RH.

Surfactant	80%	90%	95%
Tween20	0.10	0.08	0.06
Triton X-100	0.05	0.05	0.03
OTG	0.04	0.03	0.02

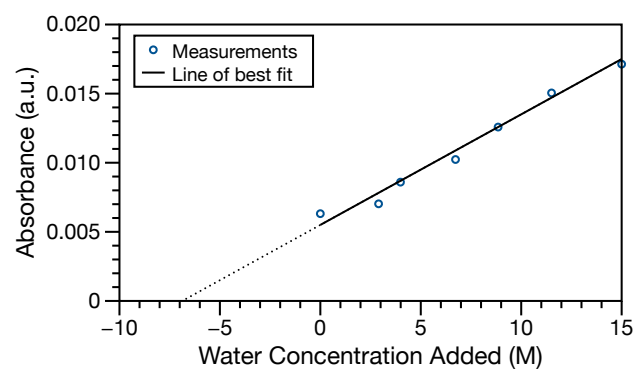


Figure S1: Standard addition calibration curve to determine the amount of water in ‘pure’ Tween20. Line of best fit:  $y = 0.0008x + 0.0055$ ,  $R^2 = 0.9818$ , and  $x$ -intercept:  $6.88 \pm 0.90$  M.

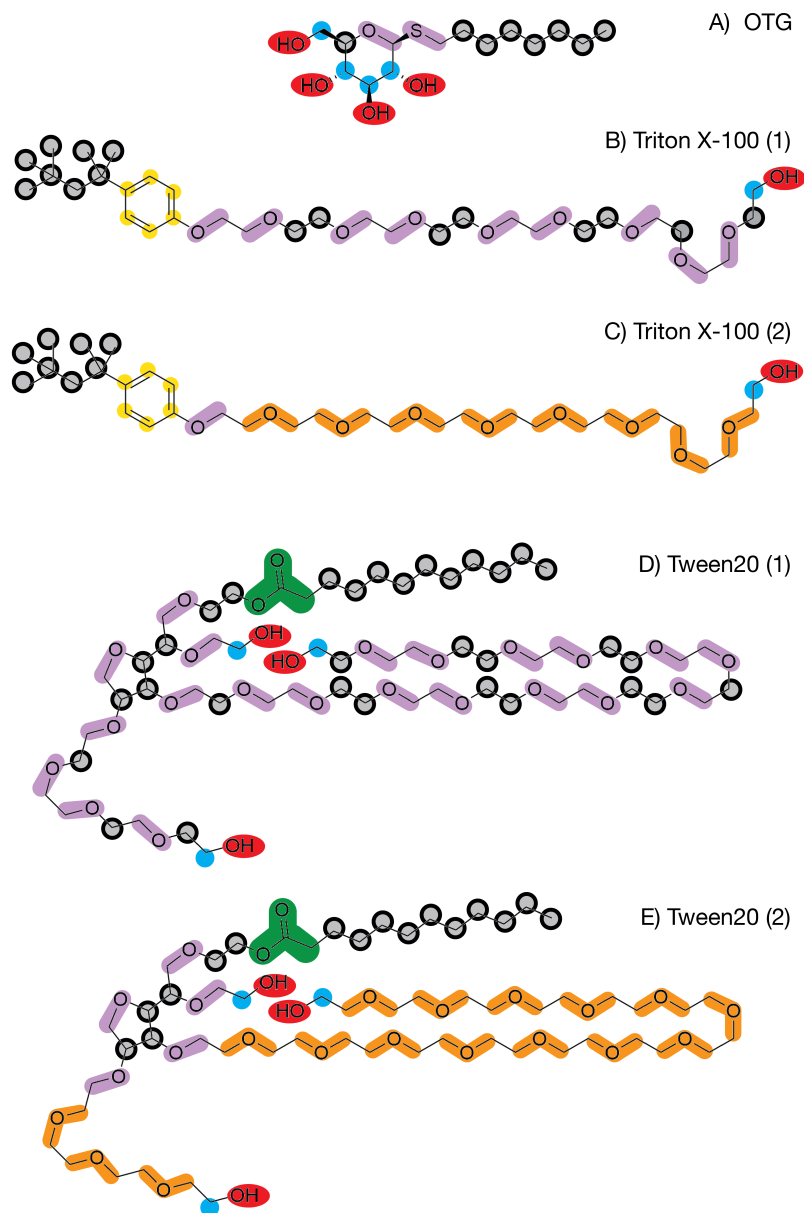


Figure S2: Nonionic surfactant structure of A) OTG, B/C) Triton X-100, and D/E) Tween20 used to determine functional subgroups for AIOMFAC calculations. OTG contains a sulfur atom, which is not currently included in any AIOMFAC organic subgroups. We have used oxygen to replace sulfur in OTG due to their shared number of valence electrons and similarity in electronegativity. Triton X-100 contains a mixture of  $\text{OCH}_2\text{CH}_2$  tail lengths with an average of 9.5 repeat units. Here we have used 9 repeat units. We find no significant difference in AIOMFAC outputs if 10 repeat units are used instead. Tween20 is a mixture of molecules with different  $\text{OCH}_2\text{CH}_2$  chain lengths at different positions. The depicted structure is one possible configuration. The length of each chain does not impact the definition of functional subgroups.

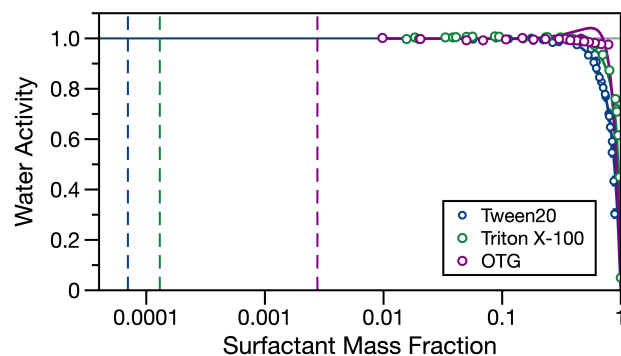


Figure S3: Water activity as a function of surfactant mass fraction plotted on a log scale, for binary surfactant solutions shown in Fig. 1 of the main text. The CMC of each surfactant is shown by the vertical dashed line in the same color as the points. The AIOMFAC model lines for each surfactant are also shown as solid lines in the same color.

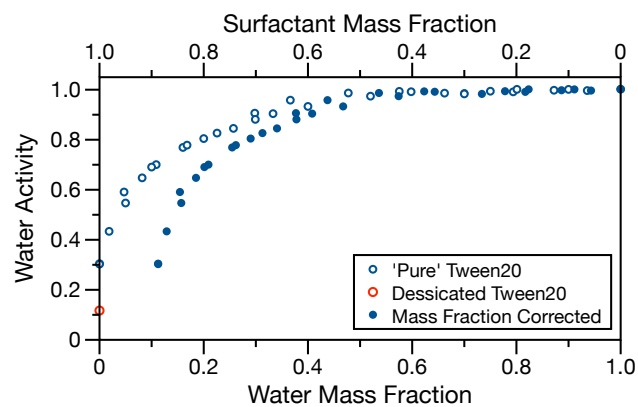


Figure S4: Water activity measurements for 'pure' Tween20 before and after mass fraction of water correction. The open red point shows the water activity of 'pure' Tween20 after a sample was left in the desiccator for a week.

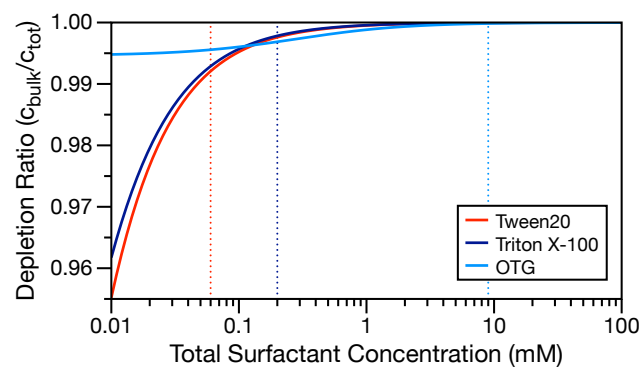


Figure S5: Predicted depletion ratios due to bulk-to-surface partitioning in an 8 mL sample using a simple kinetic partitioning model based on the Langmuir isotherm.<sup>1</sup> Vertical dotted lines in the same color indicate the CMC of each surfactant.

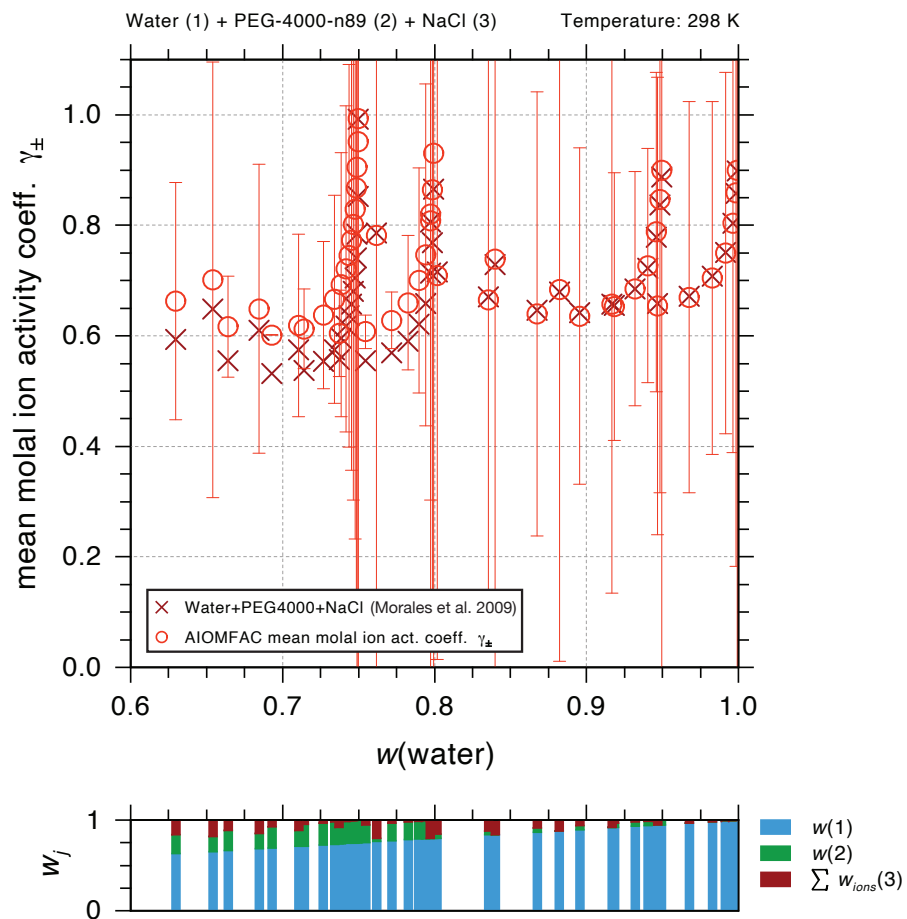


Figure S6: Mean molal ion activity coefficients for water–PEG4000–NaCl solutions predicted using an analogy to the  $\text{CH}_n\text{O}$  ether group approach in AIOMFAC to provide interaction parameters between the oxyethylene group, and  $\text{Na}^+$  and  $\text{Cl}^-$  ions, compared to those determined experimentally by Morales et al.<sup>6</sup>

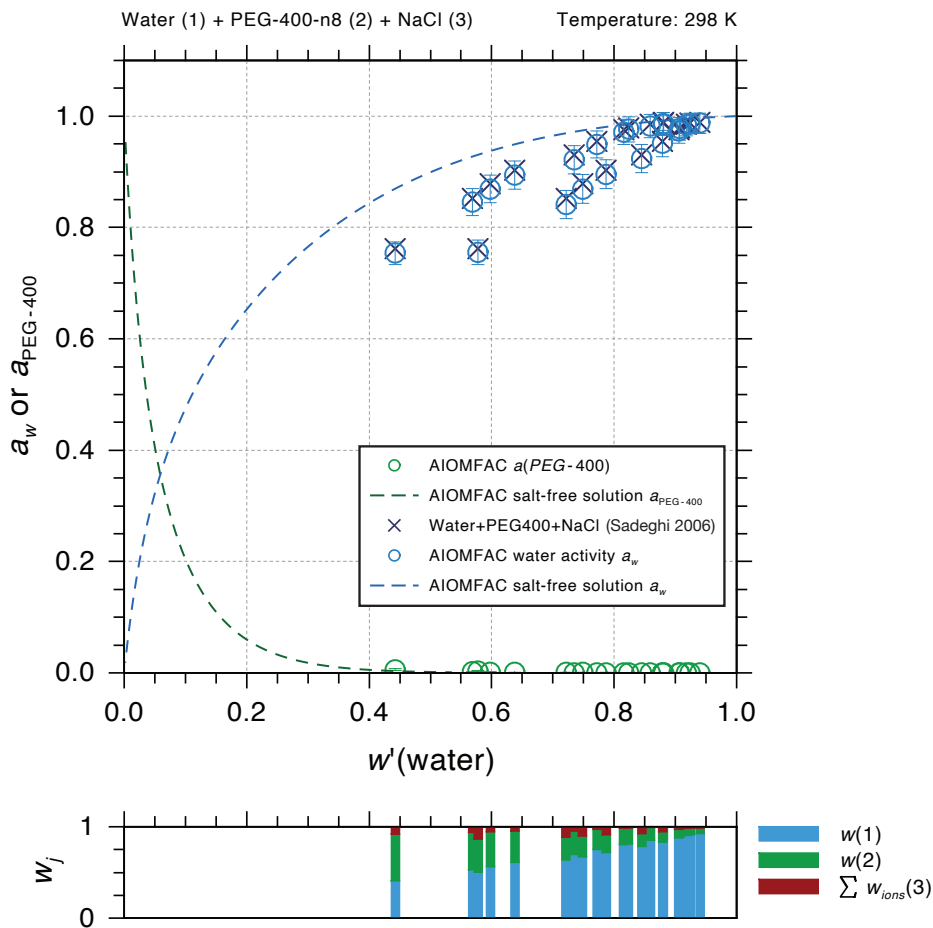


Figure S7: Water activities for water–PEG400–NaCl solutions predicted using an analogy to the  $\text{CH}_n\text{O}$  ether group approach in AIOMFAC to provide interaction parameters between the oxyethylene group, and  $\text{Na}^+$  and  $\text{Cl}^-$  ions, compared to those determined experimentally by Sadeghi and Ziamajidi.<sup>7</sup> The  $x$ -axis refers to the mass fraction of water,  $w'(\text{water})$ , of the salt-free solvent mixture, while the lower panel indicates the ternary mixture composition of each data point in mass fractions of water, PEG-400 and NaCl.

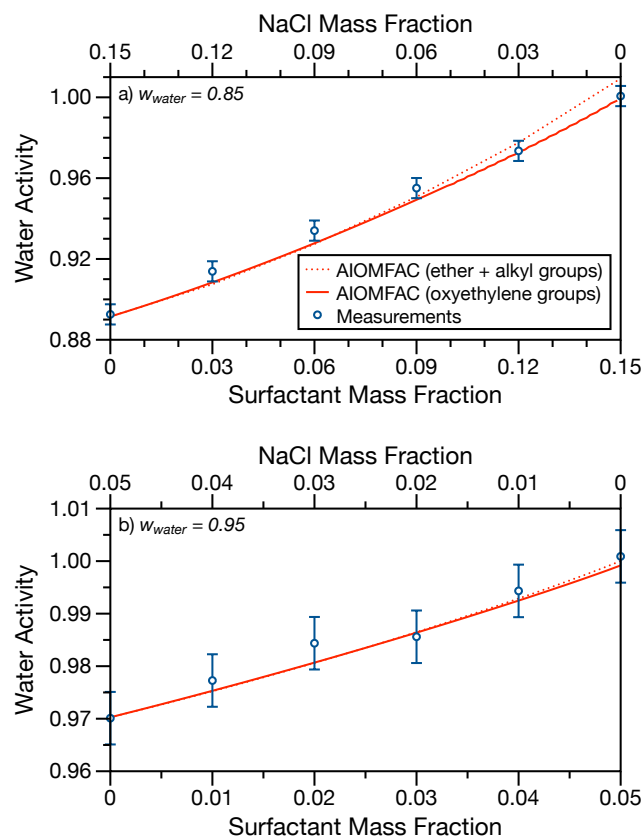


Figure S8: Water activity of aqueous solutions containing NaCl and Triton X-100, a)  $w_{water} = 0.85$  and b)  $w_{water} = 0.95$ . The mass fraction of water is held constant while the mass ratio of surfactant to NaCl is varied. The solid line shows the predictions from the online version of AIOMFAC using the oxyethylene subgroup, the dotted red line shows predictions using the ether/alkyl subgroups, and the data markers show the average of three experimental measurements. Error bars indicate the instrument precision ( $\pm 0.005$  water activity units), which is always larger than the standard deviation between measurements.

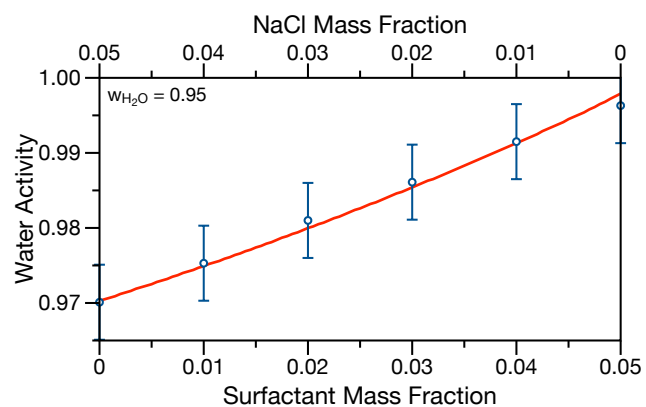


Figure S9: Water activity of aqueous solutions containing NaCl and OTG ( $w_{water} = 0.95$ ). The mass fraction of water is held constant while the mass ratio of surfactant to NaCl is varied. The solid line shows the predictions from the online version of AIOMFAC, and the data markers show the average of three experimental measurements. Error bars indicate the instrument precision ( $\pm 0.005$  water activity units), which is always larger than the standard deviation between measurements.

## 53 References

- 54 1. Alvarez, N. J.; Walker, M.; Anna, S. L. A criterion to assess the impact of confined volumes  
55 on surfactant transport to liquid–fluid interfaces. *Soft Matter* **2012**, *8*, 8917–8925.
- 56 2. Bain, A.; Prisle, N. L.; Bzdek, B. R. Model-measurement comparisons for surfactant-  
57 containing aerosol droplets. *ACS Earth Space Chem.* **2024**, *8*, 2244–2255.
- 58 3. Zdziennicka, A.; Szymczyk, K.; Krawczyk, J.; Jańczuk, B. Activity and thermodynamic  
59 parameters of some surfactants adsorption at the water-air interface. *Fluid Ph. Equilibria*  
60 **2012**, *318*, 25–33.
- 61 4. Bain, A.; Ghosh, K.; Prisle, N. L.; Bzdek, B. R. Surface-area-to-volume ratio determines  
62 surface tensions in microscopic, surfactant-containing droplets. *ACS Cent. Sci.* **2023**, *9*,  
63 2076–2083.
- 64 5. Petters, M. D.; Kreidenweis, S. M. A single parameter representation of hygroscopic growth  
65 and cloud condensation nucleus activity. *Atmospheric Chemistry and Physics* **2007**, *7*, 1961–  
66 1971.
- 67 6. Morales, J. W.; Galleguillos, H. R.; Taboada, M. E.; Hernández-Luis, F. Activity coefficients  
68 of NaCl in PEG 4000+water mixtures at 288.15, 298.15 and 308.15K. *Fluid Ph. Equilibria*  
69 **2009**, *281*, 120–126.
- 70 7. Sadeghi, R.; Ziamajidi, F. Water activities of ternary mixtures of poly(ethylene glycol), NaCl  
71 and water over the temperature range of 293.15K to 313.15K. *J. Chem. Thermo.* **2006**, *38*,  
72 1335–1343.